Transactions, SMiRT-24
BEXCO, Busan, Korea - August 20-25, 2017
Division VII

APPLICABILITY OF SPECTRAL STOCHASTIC FINITE ELEMENT METHOD TO FRAGILITY OF SLOPE STABILITY

Wataru Hotta[1], Kazumoto Haba[2], Akihito Hata[3], Shunichi Suzuki[4], Kazuaki Watanabe[5] and Muneo Hori[6]

[1] Manager, Nuclear Facilities Division, Taisei Corporation, Japan
[2] Assistant Manager, Nuclear Facilities Division, Taisei Corporation, Japan
[3] Chief Research Engineer, Technology Center, Taisei Corporation, Japan
[4] Manager, Nuclear Facilities Division, Taisei Corporation, Japan
[5] Manager, Nuclear Facilities Division, Taisei Corporation, Japan
[6] Professor, Earthquake Research Institute, Tokyo University, Japan

ABSTRACT

Probabilistic analysis is an essential element in seismic safety assessment after the accidents of Fukushima Daiichi nuclear power plant. Spectral Stochastic Finite Element Method (SSFEM) is an alternative to Monte-Carlo Simulation (MCS) as the probabilistic analysis method, as it is able to calculate various probabilistic characteristics in relatively low computational cost.

This paper examines the applicability of SSFEM to the fragility assessment of slopes subjected to earthquake ground motion. A dynamic SSFEM is developed to this end, and numerical experiments are carried out. It is shown that SSFEM has almost the same accuracy with the conventional MCS, reducing numerical computation drastically compared with MCS.

INTRODUCTION

It is important to accurately estimate soil properties in earthquake engineering, for reasonably accurate seismic design. However, soil properties are inhomogeneous and need to be presumed by a limited number of in-situ tests, boring tests or seismic surveys, and a certain uncertainty is inevitably included. The assessment of such uncertainty of soil properties is essential in adopting a performance based design and a reliability based design method to practical structural design, or Probabilistic Risk Assessment (PRA) to nuclear power plants.

The authors are studying the effects of the spatial variability of soil properties on the seismic ground response by using Spectral Stochastic Finite Element Method (SSFEM), which has an advantage over Monte-Carlo Simulation (MCS) in terms of computational cost; SSFEM is able to calculate probabilistic characteristics at once, unlike MCS which requires repetitive realizations of a stochastic model.

Although it is efficient, limited application has been made for SSFEM to evaluate the effects of uncertainty of soil properties. The reason is simple. Only soil stiffness is regarded as a random variable in SSFEM, and non-linearity of soil properties is out of application of SSFEM; see Anders and Hori (1999, 2001) and Sett, Jeremic and Kavvas (2011) for the use of SSFEM to the non-linear problems. An efficient treatment of non-linear elasto-plasticity is needed for SSFEM. Another limitation of SSFEM is large computational cost. Even though MCS needs much more computation, SSFEM needs a larger amount of numerical computation compared with an ordinary FEM. This problem, however, is readily solved by enhancing SSFEM with parallel computing capability; a solver of SSFEM is updated with an appropriate algorithm.

The present study is undertaken in order to examine the applicability of SSFEM to the fragility assessment of seismic slope stability. Presented is a dynamic SSFEM, in which a solver that uses the conjugate gradient method for scalable parallel computing are implemented. A numerical experiment is carried out, to evaluate ground failure probability (which is illustrated by the Atomic Energy Society of Japan (2015)) by using the developed dynamics SSFEM.

OVERVIEW OF SSFEM

SSFEM was proposed by Ghanem and Spanos (1991) who applied Karhunen-Loeve expansion (KL expansion) and Polynomial Chaos expansion (PC expansion) for stochastic material properties and field variables respectively. Using these two expansions, it has the feature which can calculate various probabilistic characteristics such as mean, variance and probability density function with considered spatial variability of soil properties, at once, which is without any repetitive calculations. It should be noted that only soil stiffness (ex. Young's module or shear modulus) is taken as a random variable in this paper based on the paper by Ghanem and Spanos (1991).

KL Expansion of Input Data

First, Young's module E can be defined as

$$E(\boldsymbol{x},\omega) = < E > \{1+\alpha(\boldsymbol{x},\omega)\} \tag{1}$$

where $< E >$ is a mean value, x is a coordinate of the target position and ω is a sample point of sample space. When the covariance function of $\alpha(\boldsymbol{x},\omega)$ is given as $C(\boldsymbol{x}_1,\boldsymbol{x}_2)$, we can obtain the following KL expansion:

$$\alpha(\boldsymbol{x},\omega) = \sum_{n=1}^{\infty} \sqrt{\lambda_n}\phi_n(\boldsymbol{x})\xi_n(\omega) \tag{2}$$

$$\int C(\boldsymbol{x}_1,\boldsymbol{x}_2)\phi_n(\boldsymbol{x}_2)d\boldsymbol{x}_2 = \lambda_n\phi_n(\boldsymbol{x}_1) \quad n=1, 2, 3, \dots \tag{3}$$

where λ_n and $\phi_n(\boldsymbol{x})$ are the eigenvalue and eigenvector of $C(\boldsymbol{x}_1,\boldsymbol{x}_2)$ respectively, and the zero-mean random variables, $\xi_n(\omega)$ are mutually independent and have unit variances.

PC Expansion of Output

Response of displacement $\boldsymbol{u}(\boldsymbol{x},\omega)$ is represented by PC expansion, which is expressed as

$$\boldsymbol{u}(\boldsymbol{x},\omega) = \boldsymbol{u_0}\Gamma_0 + \sum_{i1=1}^{\infty}\boldsymbol{u_{i1}}\Gamma_1(\xi_{i1}) + \sum_{i1=1}^{\infty}\sum_{i2=1}^{i1}\boldsymbol{u_{i1i2}}\Gamma_2(\xi_{i1},\xi_{i2}) + \sum_{i1=1}^{\infty}\sum_{i2=1}^{i1}\sum_{i3=1}^{i2}\boldsymbol{u_{i1i2i3}}\Gamma_3(\xi_{i1},\xi_{i2},\xi_{i3}) + \dots \tag{4}$$

where $\Gamma_n(\cdot)$ is multidimensional Hermite polynomial, which is defined as

$$\Gamma_n(\xi_{i1},\dots,\xi_{in}) = e^{\frac{1}{2}\xi^T\xi}(-1)^n\frac{\partial^n}{\partial\xi_{i1}\dots\partial\xi_{in}}e^{-\frac{1}{2}\xi^T\xi} \quad \boldsymbol{\xi} = (\xi_{i1},\dots,\xi_{in})^T \tag{5}$$

Eq. (4) is easily expressed as

$$\boldsymbol{u}(\boldsymbol{x},\omega)=\sum_{i=0}^{\infty}\boldsymbol{u}_i\Psi_i[\{\xi\}] \tag{6}$$

where $\Psi_i[\{\xi\}]$ corresponds to function of $\Gamma_n(\cdot)$ with various ξ. Furthermore, the orthogonality of PC is taken into consideration, which is defined as

$$<\Psi_i[\{\xi\}]\Psi_j[\{\xi\}]>=\delta_{ij} \tag{7}$$

where δ_{ij} is Kronecker delta.

Overview of Dynamic SSFEM

Now, we summarize the basic procedure to solve a stochastic matrix equation of dynamic SSFEM. Rayleigh damping is assumed, and a stiffness proportional part of Rayleigh damping is treated as a random variable.

The stochastic matrix equation of dynamic SSFEM is formally expressed as

$$\boldsymbol{M}\boldsymbol{a}(\boldsymbol{x},\omega)+\boldsymbol{C}(\boldsymbol{x},\omega)\boldsymbol{v}(\boldsymbol{x},\omega)+\boldsymbol{K}(\boldsymbol{x},\omega)\boldsymbol{u}(\boldsymbol{x},\omega)=\boldsymbol{p}(x) \tag{8}$$

where $\boldsymbol{M}$, $\boldsymbol{C}(x,\omega)$ and $\boldsymbol{K}(x,\omega)$ are a mass, a damping and a stiffness matrix, and $\boldsymbol{a}(x,\omega)$, $\boldsymbol{v}(x,\omega)$ and $\boldsymbol{u}(x,\omega)$ are an acceleration, a velocity and a displacement vector respectively. Also $\boldsymbol{p}(x)$ is an external force vector. $\boldsymbol{M}$ and $\boldsymbol{p}(x)$ are deterministic and others are stochastic. Here, arguments t which express time are omitted. By using KL expansion, the damping matrix is expressed as

$$\boldsymbol{C}(\boldsymbol{x},\omega)=\sum_{n=0}^{\infty}\boldsymbol{C}^{(n)}\xi_n \tag{9}$$

and

$$\boldsymbol{C}^{(n)}=\begin{cases} a\boldsymbol{M}+b\boldsymbol{K}^{(0)}\,(n=0) \\ b\boldsymbol{K}^{(n)}\,(n\neq 0)\end{cases} \tag{10}$$

where a and b are coefficients and $\boldsymbol{C}^{(0)}$ and $\boldsymbol{K}^{(0)}$ are defined as means.

By using PC expansion given in Eq. (6), $\boldsymbol{a}(x,\omega)$ and $\boldsymbol{v}(x,\omega)$ are expressed as

$$\boldsymbol{a}(\boldsymbol{x},\omega)=\sum_{i=0}^{\infty}\boldsymbol{a}_i\Psi_i[\{\xi\}] \tag{11}$$

$$\boldsymbol{v}(\boldsymbol{x},\omega)=\sum_{i=0}^{\infty}\boldsymbol{v}_i\Psi_i[\{\xi\}] \tag{12}$$

Here, considering that $\Psi_i[\{\xi\}]$ doesn't depend on time, a_i and v_i are expressed as

$$\boldsymbol{a}_i = \frac{d^2}{dt^2}\boldsymbol{u}_i \quad \boldsymbol{v}_i = \frac{d}{dt}\boldsymbol{u}_i \tag{13}$$

We can rewrite Eq. (8) given in Eq. (6), Eq. (9), Eq. (11), Eq. (12) and the stiffness matrix using KL expansion as

$$\boldsymbol{M}\sum_{i=0}^{\infty}\boldsymbol{\alpha}_i\Psi_i[\{\xi\}] + \sum_{n=0}^{\infty}\boldsymbol{C}^{(n)}\xi_n\sum_{i=0}^{\infty}\boldsymbol{v}_i\Psi_i[\{\xi\}] + \sum_{n=0}^{\infty}\boldsymbol{K}^{(n)}\xi_n\sum_{i=0}^{\infty}\boldsymbol{u}_i\Psi_i[\{\xi\}] = \boldsymbol{p} \tag{14}$$

Galerkin type procedure may be applied to Eq. (14) to solve for the unknown coefficients $\boldsymbol{a}(x,\omega)$, $\boldsymbol{v}(x,\omega)$ and $\boldsymbol{u}(x,\omega)$. One may write Eq. (14) as (cf. Ghanem and Spanos (1991))

$$\begin{aligned}&\boldsymbol{M}\boldsymbol{\alpha}_j + \sum_{i=0}^{\infty}\boldsymbol{v}_i\sum_{n=0}^{\infty} < \xi_n\Psi_i[\{\xi\}]\Psi_j[\{\xi\}] > \boldsymbol{C}^{(n)} \\ &+ \sum_{i=0}^{\infty}\boldsymbol{u}_i\sum_{n=0}^{\infty} < \xi_n\Psi_i[\{\xi\}]\Psi_j[\{\xi\}] > \boldsymbol{K}^{(n)} = < \boldsymbol{p}\Psi_j[\{\xi\}] >\end{aligned} \tag{15}$$

Eq. (15) can be rewritten as

$$\boldsymbol{M}\boldsymbol{\alpha}_j + \sum_{i=0}^{\infty}\boldsymbol{C}_{ij}\boldsymbol{v}_i + \sum_{i=0}^{\infty}\boldsymbol{K}_{ij}\boldsymbol{u}_i = \boldsymbol{p}_j \tag{16}$$

where

$$\boldsymbol{C}_{ij} = \sum_{n=0}^{\infty} < \xi_n\Psi_i[\{\xi\}]\Psi_j[\{\xi\}] > \boldsymbol{C}^{(n)} \tag{17}$$

$$\boldsymbol{K}_{ij} = \sum_{n=0}^{\infty} < \xi_n\Psi_i[\{\xi\}]\Psi_j[\{\xi\}] > \boldsymbol{K}^{(n)} \tag{18}$$

$$\boldsymbol{p}_j = < \boldsymbol{p}\Psi_j[\{\xi\}] > \tag{19}$$

Next, we show the numerical time integration method. Here, Newmark β method (β=0.25 and γ=0.5) is used as the implicit method. The time interval Δt is shown in subscript m, and the formulation updating from $t=t^m$ to $t=t^{m+1}$ is considered. Then, the displacement and velocity vector are expressed as

$$\boldsymbol{v}_i^{m+1} = \boldsymbol{v}_i^m + \frac{\Delta t}{2}\boldsymbol{a}_i^m + \frac{\Delta t}{4}\boldsymbol{a}_i^{m+1} \tag{20}$$

$$\boldsymbol{u}_i^{m+1} = \boldsymbol{u}_i^m + \Delta t\boldsymbol{v}_i^m + \frac{\Delta t^2}{4}\boldsymbol{a}_i^m + \frac{\Delta t^2}{4}\boldsymbol{a}_i^{m+1} \tag{21}$$

The displacement, velocity and acceleration vector are calculated by substituting Eq. (20) and Eq. (21) given in Eq. (16) at the time of $t=t^{m+1}$. Therefore, Eq. (15) can be computed as the second order differential equation as with the normal dynamic equation of motion. Here, expansion order of Eq. (15) is aborted by finite values.

The size of the mass, damping and stiffness matrix are bigger than the size of deterministic FEM, corresponding to the probability component. Then, it is important for SSFEM to deal with the matrix manipulation effectively using parallel computing and appropriate algorithms for large-scale models, for example Matrix Jacobi Method suggested by Anders and Hori (2001).

FRAGILITY OF SLOPE STABILITY USING SSFEM

Method of Assessment

In this section, an applicability is tested using SSFEM to the assessment method of ground failure probability illustrated by AESJ PRA guideline (2015), and is verified by comparing with MCS results. Especially, the results suggest that SSFEM is a computationally efficient method that can guarantee the same accuracy with conventional MCS and also reduce calculation time compared with MCS.

Both methods of assessment of ground failure probability illustrated in AESJ PRA guideline and a new method using SSFEM are shown in Fig. 1. The method using SSFEM is almost the same as the original method in terms of process of calculating resisting force and sliding force by initial stress analysis and seismic response analysis. But it should be pointed out that we can calculate the failure probability by one seismic response analysis, while the original method need the same number of seismic response analysis with sampling points of targeted parameters. Uncertain parameters in this study are defined as shear modulus and cohesion, because some studies have reported that these two parameters affect the ground failure probability of slope compared with other parameters through sensitivity analysis.

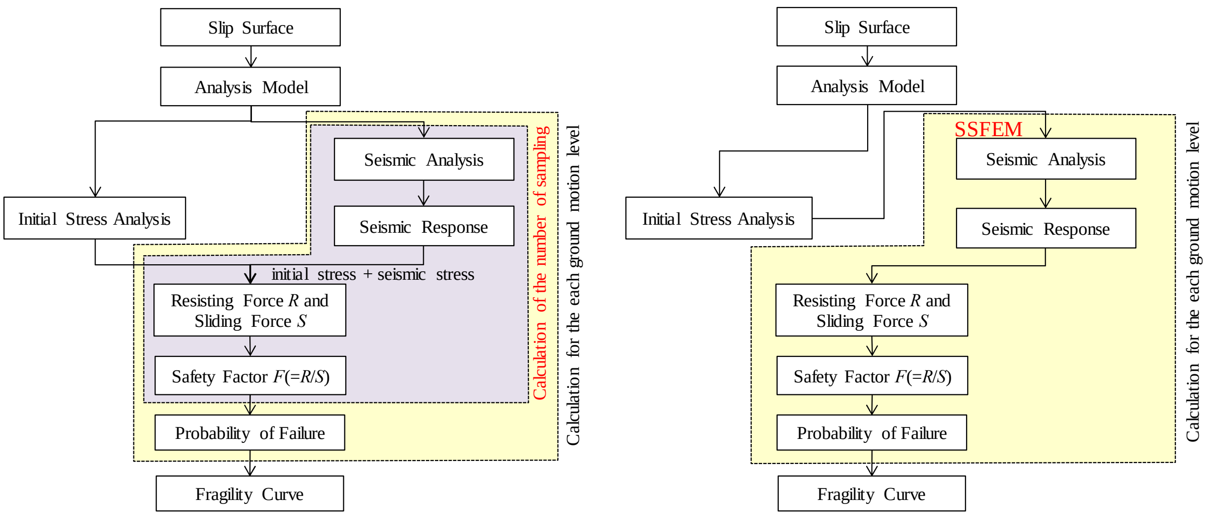

(a) Original method (b) New method

Figure 1. Flow of assessment of ground failure probability.

Calculation Procedure of Fragility

SSFEM results are expressed in polynomials including random variables. For example, a node displacement is expressed as a polynomial and consequently an element strain can be calculated as the gradient of the displacement. By multiplying mean of young modulus, a polynomial of an element stress is expressed as

$$
\begin{aligned}
s_{xx}(x,\omega) &= \sum_{\alpha=0}^{P} \Psi_\alpha[\{\xi\}] s_{xx}^{(\alpha)}(x) \\
s_{yy}(x,\omega) &= \sum_{\alpha=0}^{P} \Psi_\alpha[\{\xi\}] s_{yy}^{(\alpha)}(x) \\
s_{xy}(x,\omega) &= \sum_{\alpha=0}^{P} \Psi_\alpha[\{\xi\}] s_{xy}^{(\alpha)}(x)
\end{aligned}
\tag{22}
$$

Vertical stress $\sigma_n(x,\omega)$ and shear stress $\tau_n(x,\omega)$ of an element on the slip surface are expressed as

$$\sigma_n(x,\omega) = \frac{s_{xx}(x,\omega)+s_{yy}(x,\omega)}{2} + \frac{s_{xx}(x,\omega)-s_{yy}(x,\omega)}{2}\cos 2\varphi + s_{xy}(x,\omega)\sin 2\varphi \tag{23}$$

$$\tau_n(x,\omega) = \frac{s_{xx}(x,\omega)-s_{yy}(x,\omega)}{2}\sin 2\varphi - s_{xy}(x,\omega)\cos 2\varphi \tag{24}$$

where φ is an angle between normal direction of the slip surface and direction of x. Cohesion $c(\omega')$ is assumed the normal distribution. Correlation between cohesion and shear modulus is not taken into consideration, and cohesion and shear modulus of the slip surface are fluctuated evenly.

Resisting force R and sliding force S are expressed as

$$R(x,\omega) = \int \{c(\omega') + \sigma_n(x,\omega)\tan\phi\}dx = R_1(\omega') + R_2(x,\omega) \tag{25}$$

$$S(x,\omega) = \int \tau_n(x,\omega)dx \tag{26}$$

where ϕ is a friction angle and dx is an element length. Furthermore, these two parameters are deterministic. In Eq. (25), the member of cohesion $R_1(\omega)$ and the member of vertical stress $R_2(x,\omega)$ are independent of each other.

Safety factor of slope stability F is expressed as

$$F(x,\omega) = R(x,\omega)/S(x,\omega) \tag{27}$$

Both numerator and denominator in Eq. (27) are probabilistic functions. Therefore, we use MCS to solve the safety factor of slope stability efficiently. ξ and random variable of cohesion are generated as random number N based on the normal distribution, and substituted in Eq. (25) and Eq. (26). As a result, N safety factor of slope stability could be calculated. Furthermore, means, standard deviations and probability density functions of safety factor could be calculated by the process of statistic. Finally, we consider the probability that safety factor is 1 or less as failure probability.

Example Problem

The slope stability model is shown in Figure 2. Shear modulus of soil is assumed to be a Gaussian random field, and the coefficients of variation range from COV_G=0.1 to 0.3. The covariance function is shown as

$$C(x_1,y_1,x_2,y_2) = (COV_G)^2 \exp\left(-\frac{|x_2-x_1|}{\theta_x} - \frac{|y_2-y_1|}{\theta_y}\right) \tag{28}$$

where the correlation lengths range from $\theta x=\theta y$=1m to 100m. Similarly, cohesion of soil is assumed to be a Gaussian random field, and the coefficients of variation range from COV_c=0.0 to 0.2; see Table 1. A slip surface through toe of slope is assumed. Seismic motion is shown in Figure 3; shown by Standard Specifications for Concrete Structures of JSCE, and it is input to the horizontal direction. The number of terms of KL expansion is M and PC expansion is p, and the impact of those numbers are checked thorough parameters studies. MCS random field of soil parameters is generated using Fourier series expansion proposed by Hata and Shiba (2010) and 1,000 realizations of MCS are conducted.

Time history data of means $\langle F \rangle$ and standard deviations S.D.(F) of safety factor of slope stability using both SSFEM and MCS is shown in Figure 4. The number of terms of KL expansion and PC expansion are M=3 and p=1 respectively. The data using SSFEM is quite similar to the data using MCS. Next, probability density function (PDF) of safety factor, at the time which a mean of safety factor is minimized (t=8.38sec), is shown in Figure 5. PDF result using SSFEM agrees in satisfying manner with the result of MCS irrespective of the number of terms of KL expansion and PC expansion. The number of terms of KL expansion affects the accuracy of PDF more than PC expansion. The reason is that the probability distribution of response is near the normal distribution for the most part, because foundation is modelled by linear elastic solid.

Computational time required for the analysis is shown in Table 2; with 100 times of MCS is set as 1. The result of the case of M=3, p=3 is longer than the result of 1,000 times of MCS, however the results of the other cases show the one third or less compared with 1,000 times of MCS. Data consumption of 1,000 times of MCS directly requires 1,000 times of corresponding deterministic FEM. On the other hand, Data consumption of SSFEM depends on the number of terms of KL expansion and PC expansion. For example, when the number of terms of KL expansion and PC expansion are M=3 and p=1 respectively, data consumption of SSFEM requires 4 times of corresponding deterministic FEM. In addition, time consumption of SSFEM is significantly reduced by using the appropriate conjugate gradient method for scalable parallel computing. For example, we are using Matrix Jacobi Method (2001). Therefore, SSFEM is quite evident to reduce calculation time compared with MCS.

Figure 6 shows the coefficients of variation of safety factor of slope stability for different COV_G, COV_c and θ using SSFEM. When the correlation lengths are $\theta x=\theta y$=1m, the coefficients of variation of safety factor are about 0.1 without depending on the range of COV_G from Figure 6 (a). This agrees with COV_c in that the variability of soil strength is dominant. Meanwhile, the bigger the correlation lengths become, the bigger the coefficients of variance of safety factor also become. Then the influence by the difference in the COV_G could be confirmed. Figure 6 (B) also shows the same trend. The variability of soil strength is dominant when the correlation lengths are $\theta x=\theta y$=1m. On the other hand, the bigger the correlations length become, the more dominant the variability of soil stiffness is. These results indicate that it is important for the fragility assessment of seismic slope stability to research the correlation lengths accurately. Furthermore, it should be noted that these results using SSFEM correspond to the results of MCS which require a large amount of sampling.

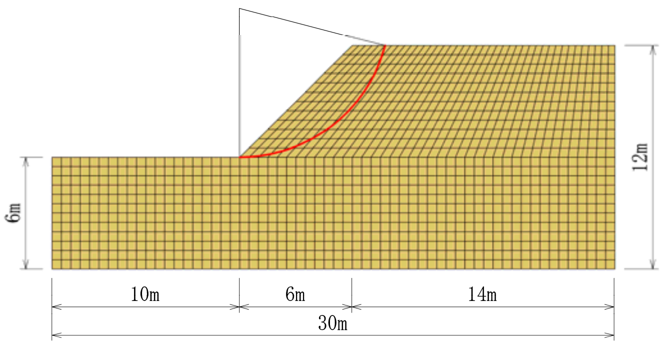

Figure 2. FEM model of the homogeneous slope.

Table 1: Statistical properties of soil parameters.

Unit Weight γ	kN/m^3	20
Shear Modulus *Go*	MPa	180
Poisson's Ratio ν	-	0.45
Damping Ratio *h*	%	3.0
Cohesion *c*	kN/m^2	40
Friction Angle ϕ	°	15
Coefficient of Variation of *Go* COV_G	-	0.1～0.3
Coefficient of Variation of *c* COV*c*	-	0.0～0.2
Correlation Length θx ,θy	m	1～100

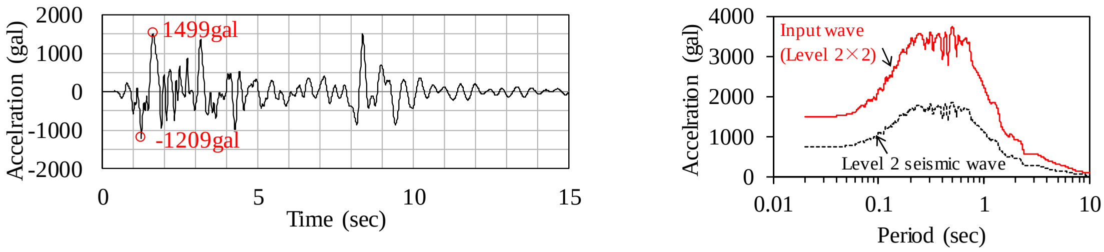

(a) Time history (b) Spectra

Figure 3. Input seismic motion.

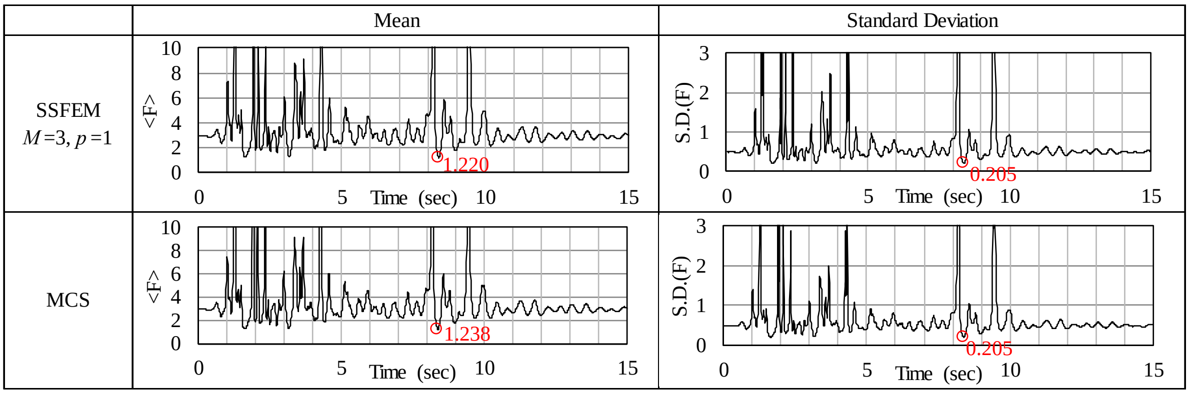

Figure 4. Time history of safety factor of slope stability: COV_G=0.3, COVc=0.2, θ=1m.

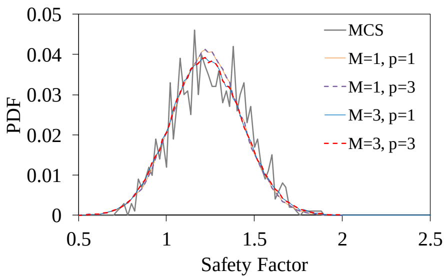

Figure 5. Probability density function of safety factor of slope stability: COV_G=0.3, COVc=0.2, θ=1m.

Table 2: Time consumption.

MCS 100 times	MCS 1,000 times	SSFEM M=1, p=1	SSFEM M=1, p=3	SSFEM M=3, p=1	SSFEM M=3, p=3
1	10	1 or less	3	3	12

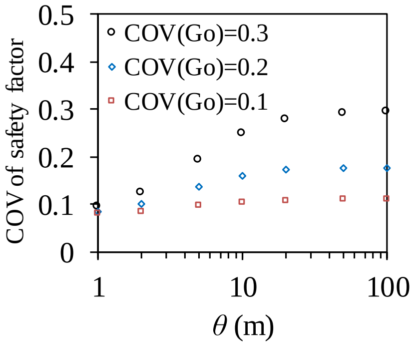

(a) COVc=0.1

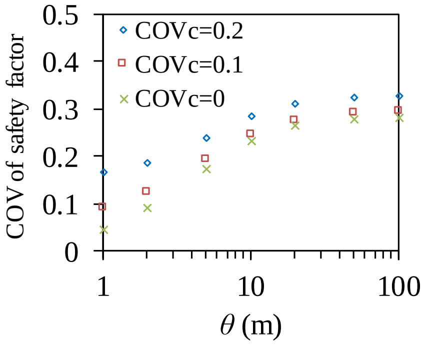

(b) COV$_G$=0.3

Figure 6. Coefficients of variation of safety factor of slope stability using SSFEM.

CONCLUSION

This paper discusses the applicability of SSFEM to the fragility assessment of seismic slope stability. The results suggest that SSFEM is a computationally efficient method that can guarantee the same accuracy with conventional MCS and also reduce calculation time compared with MCS. It is evident that SSFEM could be an alternative method for MCS in the field of Seismic PRA with respect to the limited condition. A further study of the applicability of non-liner SSFEM to various situations should be conducted.

REFERENCES

Anders, M. and Hori, M. (1999). “Stochastic finite element method for elasto-plastic body,” *Int. J. Numer. Methods Eng.*, Vol.46, No.11, pp.1897-1916.

Anders, M. and Hori, M. (2001). “Three-dimensional stochastic finite element method for elasto-plastic bodies,” *Int. J. Numer. Methods Eng.,* Vol.51, No.4, pp.449-478.

A standard for Procedure of Seismic Probabilistic Risk Assessment (PRA) for nuclear power plants. (2015). AESJ, Japan.

Ghanem, R. G. and Spanos, P. D. (1991). *Stochastic Finite Elements -A Spectral Approach-*, Springer-Verlag, Berlin.

Hata, A. and Shiba, Y. (2010). “A fundamental study on the effect of spatial variability of soil properties to earthquake responses of subsurface ground,” *Journal of Structural Engineering and Earthquake Engineering, JSCE*, Vol.66, No.1, pp.73-83.

Honda, R. (2001). “Analysis of wave propagation in random media by spectral stochastic finite element method,” *Journal of Structural Engineering and Earthquake Engineering, JSCE*, No.689, I-57, pp.321-331.

Sett, K., Jeremic, B. and Kavvas, M. L. (2011). “Stochastic Elastic-Plastic Finite Elements,” *Comput. Methods Appl. Mech. Eng.*, Vol.200, No.9-12, pp.997-1007.